



POLITECNICO
MILANO 1863

RE.PUBLIC@POLIMI

Research Publications at Politecnico di Milano

Post-Print

This is the accepted version of:

G. Bressan, A. Russo, D. Invernizzi, M. Giurato, S. Panza, M. Lovera
Adaptive Augmentation of the Attitude Control System for a Multirotor Unmanned Aerial Vehicle
Proceedings of the Institution of Mechanical Engineers, Part G: Journal of Aerospace Engineering, In press - Published online 27/12/2018
doi:10.1177/0954410018820193

The final publication is available at <https://doi.org/10.1177/0954410018820193>

Access to the published version may require subscription.

When citing this work, cite the original published paper.

Permanent link to this version

<http://hdl.handle.net/11311/1078215>

Adaptive augmentation of the attitude control system for a multirotor UAV

Journal Title
XX(X):1-8
©The Author(s) 2016
Reprints and permission:
sagepub.co.uk/journalsPermissions.nav
DOI: 10.1177/ToBeAssigned
www.sagepub.com/



G. Bressan¹, A. Russo¹, D. Invernizzi¹, M. Giurato¹, S. Panza¹, and M. Lovera¹

Abstract

In this paper the adaptive augmentation of the attitude control system for a multirotor Unmanned Aerial Vehicle (UAV) is considered. The proposed approach allows to combine a baseline controller with an adaptive one and to disable or enable the adaptive controller when needed, in order to take the advantages of both controllers. To improve transient performance with respect to the standard Model Reference Adaptive Controller (MRAC), an observed-based approach is exploited. The adaptation law is based on the error between the output of an observer of the nominal closed-loop dynamics and the actual output of the system with uncertainties. Experimental results obtained by testing the proposed approach on a quadrotor UAV are presented to compare the performance, in terms of disturbance rejection, with respect to the baseline controller and to a \mathcal{L}_1 adaptive augmentation scheme.

Keywords

UAV, Multirotor, Adaptive control, \mathcal{L}_1 augmentation, MRAC

Introduction

The problem of attitude control law design for multirotor Unmanned Aerial Vehicles (UAVs) has been studied extensively in the literature. When dealing with nominal operation, fixed-gain linear or nonlinear controllers typically suffice to solve the problem in a satisfactory way¹. If more challenging questions such as, *e.g.*, actuator degradation and faults, severe external disturbances, parameter uncertainties and time delays, are to be considered, then more advanced approaches are needed. Adaptive control is an attractive candidate to face the mentioned disturbances and uncertainties for fault-tolerant or reconfigurable unmanned flight because of its capability of learning whilst operating.

Model reference adaptive control (MRAC) is the most widely known adaptive control technique and there are many interesting results in the control of multirotor UAVs. A common characteristic of MRAC schemes is the use of a baseline controller, usually a PI controller designed by means of LQR^{2,3}, which is used to define the reference model. Both references^{2,3} show the superior performance of the augmented adaptive controller over the baseline one, in case of actuator and mass uncertainties, respectively. On the other hand, the standard MRAC approach is characterized by an inherent trade-off between good tracking performance and transient oscillations⁴. To overcome such undesired behavior, Combined/Composite direct and indirect MRAC (CMRAC) was proposed^{5,6}, which has demonstrated significant improvement of transient performance using filtered control input and state, thereby allowing higher adaptive gains with smoother parameter estimates. Closed-loop MRAC⁷, which uses closed-loop reference models, was introduced to reach the same goal. In the last decade, \mathcal{L}_1 adaptive control has emerged as a viable strategy to handle systems characterized by rapidly varying uncertainties and it has been validated experimentally in

several aerospace applications (see, *e.g.*^{8,9}). By including a low-pass filter in the scheme, a band-limited control signal is guaranteed, which allows fast adaptation rate, limited only by the available computational power. An \mathcal{L}_1 adaptive output feedback control design, tuned by minimizing a cost function based on the characteristics of the reference model and the low-pass filter, has been also proposed¹⁰. Flight test results showed that the augmented \mathcal{L}_1 adaptive system exhibits definite performance and robustness improvements. A different approach¹¹ uses a nominal backstepping controller to control the attitude of a quadrotor UAV, which is successively augmented with an \mathcal{L}_1 piecewise-constant adaptive controller. Performance is visibly improved with adaptation, since fast adaptation is now possible due to the low-pass filter introduced in the \mathcal{L}_1 methodology. These works show the control designer's ability to choose large adaptation gains for fast convergence without compromising robustness. Adaptive augmentation schemes based on neural networks have also been proposed in aerospace applications¹²⁻¹⁵. The peculiarity of those schemes is the use of the concurrent learning modification, enabling a faster converge of the estimates to their true values.

In this paper, see also the preliminary results in¹⁶, the adaptive augmentation of the attitude control system for a multirotor UAV is considered. The proposed architecture can be applied to augment any baseline linear controller that guarantees asymptotic stability of the closed-loop system

¹Dipartimento di Scienze e Tecnologie Aerospaziali, Politecnico di Milano, Italy

Corresponding author:

Marco Lovera, Dipartimento di Scienze e Tecnologie Aerospaziali, Politecnico di Milano - Via La Masa 34, 20156 Milano, Italy.

Email: marco.lovera@polimi.it

in nominal conditions. With respect to standard model reference approaches^{2,3}, our adaptive augmentation design does not require the explicit knowledge of the baseline controller structure, but only of the controller output. The approach allows to combine a baseline controller with an adaptive one and to disable or enable the adaptive controller when needed, in order to take the advantages of both controllers. The proposed adaptive scheme exploits an observer instead of a reference model and it is therefore different from the usual formulation that includes the dynamics of the reference closed-loop system. The key idea behind our strategy lies in the use of the observation error and not of the tracking error, as in the standard MRAC, to update the adaptive parameters. When the observation error is zero, either no uncertainties were present or the adaptive law has successfully compensated for them so that the system is operating in the nominal (desired) conditions. By properly tuning the observer gains, the adaptation law becomes more effective in learning the uncertainties. In this regard, our strategy, originally presented in¹⁷, is similar to the mismatched-observer based MRAC recently proposed in¹⁸, which makes use of both tracking and observation errors in adapting the parameters. Specifically,¹⁸ shows the mechanism for which the observer-based design can effectively damp transient oscillations typical of the standard MRAC while achieving tight tracking performance.

The proposed observer-like MRAC scheme has been exploited to augment the angular velocity controller of a baseline cascade attitude control architecture and it has been validated through experiments on a small quadrotor UAV. In particular, a disturbance torque, mimicking the effect of a propeller fault or a wind gust, was induced on the quadrotor in hovering conditions to compare the disturbance rejection capabilities of the observer-based MRAC with respect to the baseline controller alone. Furthermore, a modified version of the \mathcal{L}_1 controller proposed in¹¹ has been considered for comparison purposes since \mathcal{L}_1 adaptive control has been successfully flown on-board multirotor UAVs^{8,10,11}. The metrics introduced to evaluate recovery performance are the amount of time the quadrotor takes to reach level attitude after the anomaly, the peak angle deviation and the required control effort. Both the tested adaptive schemes were significantly faster in reacting to the induced disturbance compared to the baseline controller alone.

The paper is organized as follows: first the problem of adaptive augmentation is formally stated and two solutions based on MRAC and \mathcal{L}_1 adaptive control theory are presented. The proposed observer-like MRAC is thoroughly compared to a similar solution proposed in the literature. Then, the quadrotor UAV platform used in the experiment is described in detail together with the baseline controller structure. Finally, the results of the experiment carried out to measure the improvements of the proposed adaptive control system are presented and discussed.

Problem statement

The problem under study is to design an adaptive controller that can be implemented in an already existing control architecture, capable of controlling the angular velocity

dynamics of a multirotor UAV. For that purpose consider the Euler equations describing the attitude dynamics of a rigid body resolved in the principal inertial axes frame:

$$J_{xx}\dot{p} + (J_{zz} - I_{yy})qr = \ell \quad (1)$$

$$J_{yy}\dot{q} + (J_{xx} - I_{zz})pr = m \quad (2)$$

$$J_{zz}\dot{r} + (J_{yy} - I_{xx})pq = n, \quad (3)$$

where J_{xx}, J_{yy}, J_{zz} are the principal moments of inertia, $[\ell \ m \ n]^T := \tau$ represents the total torque applied to the rigid body and $[p \ q \ r]^T := \omega$ is column vector containing the components of the body angular velocity. Letting $H_0 := \text{diag}(J_{zz} - J_{yy}, J_{xx} - J_{zz}, J_{yy} - J_{xx})$ and denoting with $J_0 := \text{diag}(J_{xx}, J_{yy}, J_{zz})$ the inertia matrix, the Euler equations can be written as

$$\dot{\omega} = J_0^{-1}(\tau - H_0 f(\omega)) \quad (4)$$

where $f(\omega) := [qr \ pr \ pq]^T$. The total torque acting on a multirotor UAV can be decomposed into the sum of three contributions: aerodynamic damping torque, torque due to propellers and torque due to external disturbances. For what concerns the aerodynamic damping torque, we assume it to be proportional to ω , hence given by $A\omega$, where A is a constant uncertain matrix. The torque due to the propellers is just the control action (output of the actuators), which will be indicated by τ_c . Finally, the external disturbance torque is denoted as σ . Therefore we can write

$$\tau = A\omega + \tau_c + \sigma, \quad (5)$$

and letting $K := J_0^{-1}$, $H := KH_0$, equation (4) becomes

$$\dot{\omega} = KA\omega + K\tau_c + K\sigma + Hf(\omega). \quad (6)$$

When hovering the term $f(\omega)$ is negligible, but uncertainties and disturbances are still acting on the system, which means that the matrices K, A, H are uncertain. As for the disturbance σ , in the following we will assume it to be either constant or slowly varying. Let now the subscript 0 denote nominal values, and the subscript δ the uncertainty. Then matrices A and H can be rewritten in the following way using the additive uncertainty form:

$$A := A_0 + A_\delta, \quad H := K(H_0 + H_\delta). \quad (7)$$

On the other hand, regarding K , it is usually preferable to express the uncertainty on the input gain in multiplicative form:

$$K := K_0\Lambda_K, \quad \Lambda_K := I_3 + K_0^{-1}K_\delta, \quad (8)$$

where I_3 is the identity matrix, so that equation (4) is rewritten as

$$\dot{\omega} = K_0\Lambda_K((A_0 + A_\delta)\omega + \tau_c + \sigma) + (H_0 + H_\delta)f(\omega). \quad (9)$$

As for the actuators, their effect is modeled as a low pass filter, with constant time delay and a zero-order hold, as

$$\tau_c = G(s)u, \quad (10)$$

with

$$G(s) := \frac{1}{\tau_n s + 1} \frac{1 - e^{-st_s}}{st_s} e^{-st_s}. \quad (11)$$

Assume now that for the nominal system, *i.e.*, $A_\delta = 0, H_\delta = 0, \Lambda_K = I_3, \sigma = 0$, we design a baseline feedback controller $u_b := C_b(r, \omega)$ capable of asymptotically stabilizing the dynamics of ω , so that the DC-gain from the reference input r to ω is unitary. In addition, we suppose to be in hover, so that the term $f(\omega) \approx 0$ is negligible.

The idea behind adaptive augmentation is that we want the system to operate mainly in nominal conditions, *i.e.*, to have adaptation active only when necessary. To that purpose, let the control input u be given as

$$u := u_b + u_a, \quad (12)$$

where u_b is the control action provided by the baseline controller, while u_a is the contribution to the control action given by the adaptive controller, to be designed based on the knowledge of the nominal one. Similarly, let $\tau_c := \tau_b + \tau_a$, where $\tau_b := G(s)u_b$ and $\tau_a := G(s)u_a$.

Observer-like MRAC augmentation design of attitude control

Plant model

In the plant model

$$\dot{\omega} = K_0 \Lambda_K ((A_0 + A_\delta) \omega + \tau_b + \tau_a + \sigma) + (H_0 + H_\delta) f(\omega) \quad (13)$$

the nominal part is given by

$$K_0(A_0 \omega + \tau_b). \quad (14)$$

By adding and subtracting $K_0 A_0 \omega + K_0 \tau_b$ to the right-hand side of (13) we get

$$\begin{aligned} \dot{\omega} = K_0 \Lambda_K ((A_0 + A_\delta) \omega + \tau_b + \tau_a + \sigma) + \\ (H_0 + H_\delta) f(\omega) \pm K_0(A_0 \omega + \tau_b) = \underbrace{K_0(A_0 \omega + \tau_b)}_{\text{Nominal part}} + \\ \underbrace{K_0 \Lambda_K (\alpha_1 \omega + \alpha_2 \tau_b + \tau_a + \sigma + \alpha_3 f(\omega))}_{\text{Uncertain part}} \end{aligned} \quad (15)$$

where

$$\alpha_1 := (I_3 - \Lambda_K^{-1}) A_0 + A_\delta \quad (16)$$

$$\alpha_2 := I_3 - \Lambda_K^{-1} \quad (17)$$

$$\alpha_3 := (K_0 \Lambda_K)^{-1} (H_0 + H_\delta). \quad (18)$$

Notice that Λ_K^{-1} always exists since

$$\Lambda_K = I_3 + K_0^{-1} K_\delta > 0,$$

as K_0 is positive definite and K_δ is positive semi-definite.

Control law

Based on (15), the adaptive control law u_a is defined as

$$u_a := -\hat{\alpha}_1 \omega - \hat{\alpha}_2 \tau_b - \hat{\sigma} - \hat{\alpha}_3 f(\omega) \quad (19)$$

where $\hat{\alpha}_1$ is the estimate of α_1 , $\hat{\alpha}_2$ is the estimate of α_2 , $\hat{\sigma}$ is the estimate of σ and finally $\hat{\alpha}_3$ is the estimate of α_3 . Hence,

letting

$$\Delta \alpha_i := \hat{\alpha}_i - \alpha_i, \quad i = 1, 2, 3 \quad (20)$$

$$\Delta \sigma := \hat{\sigma} - \sigma \quad (21)$$

we get

$$\begin{aligned} \dot{\omega} = K_0(A_0 \omega + \tau_b) - K_n \Lambda_K (\Delta \alpha_1 \omega + \\ \Delta \alpha_2 \tau_b + \Delta \sigma + \Delta \alpha_3 f(\omega)) \end{aligned} \quad (22)$$

where the assumption that $\tau_a \approx u_a$ has been used for small adaptive gains.

Observer-like reference model and error dynamics

We now build an observer of the nominal part of the plant in the following way:

$$\dot{\hat{\omega}} = K_0(A_0 \hat{\omega} + \tau_b) + L e \quad (23)$$

where

$$e := \hat{\omega} - \omega \quad (24)$$

and L is a Hurwitz matrix, added to assign the error dynamics, given by:

$$\begin{aligned} \dot{e} = (K_0 A_0 + L) e + K_0 \Lambda_K (\Delta \alpha_1 \omega \\ + \Delta \alpha_2 \tau_b + \Delta \sigma + \Delta \alpha_3 f(\omega)). \end{aligned} \quad (25)$$

Matrix L can be chosen in many ways: for instance it can be found by optimizing the \mathcal{L}_∞ norm of the error e . In the following it is assumed that the solutions of the observer are globally uniformly bounded for any bounded reference signal r and any bounded observation error e . This assumption is easily satisfied for practical cases, *e.g.*, when the baseline controller is linear. In that case it is verified by requiring that the nominal closed-loop system is asymptotically stable.

Adaptive laws

Based on the control law and on the error equation, the following adaptive laws can be deduced:

$$\dot{\hat{\alpha}}_1 := \text{Proj}(\hat{\alpha}_1, -\Gamma_1 \omega e^T P B) \quad (26)$$

$$\dot{\hat{\alpha}}_2 := \text{Proj}(\hat{\alpha}_2, -\Gamma_2 \tau_b e^T P B) \quad (27)$$

$$\dot{\hat{\alpha}}_3 := \text{Proj}(\hat{\alpha}_3, -\Gamma_3 f(\omega) e^T P B) \quad (28)$$

$$\dot{\hat{\sigma}} := \text{Proj}(\hat{\sigma}, -\Gamma_4 e^T P B) \quad (29)$$

where $\text{Proj}(\cdot, \cdot)$ is the projection operator⁴ and the initial conditions are set to $\hat{\alpha}_1(0) = \hat{\alpha}_2(0) = 0$, $\hat{\sigma}(0) = 0$ and $\hat{\alpha}_3(0) = K_0^{-1} H_0$. The symmetric matrix P is chosen so as to satisfy the Lyapunov equation:

$$A_e^T P + P A_e = -Q, \quad A_e := K_0 A_0 + L, \quad (30)$$

where $Q = Q^T > 0$ was chosen as $Q = I_3$. Note that by selecting a gain of the form $L = -k_L I_3$, where k_L is a positive scalar, the only non-null components of $\hat{\alpha}_i$ are the diagonal ones, thereby reducing significantly the order of the controller.

The proof of convergence of the observation error can be derived along the lines of the proof of [Theorem 1]⁷, by first proving that the observation error is uniformly bounded (from which it follows that all the signals of the closed-loop system are uniformly bounded thanks to the boundedness assumption on the observer solutions) and finally by invoking Barbalat's Lemma, according to consolidated proof techniques in adaptive control.

Comparison with the mismatched-observer based adaptive design of Kim¹⁸

As mentioned in the Introduction, an observer-based MRAC scheme has been recently proposed with the aim of improving transient performance of standard MRAC. The underlying development follows a similar reasoning to the one of our strategy and it is therefore interesting to point out how the two schemes are related. Specifically, in¹⁸ the observation error is defined as

$$e := k_L(e_t - e_{t_f}), \quad (31)$$

where $e_t := \omega - \omega_r$ is the tracking error employed in the standard MRAC approach and e_{t_f} is a corresponding filtered version, the dynamics of which is assigned as:

$$\dot{e}_{t_f} := A_r e_t + k e \quad (32)$$

in which A_r is the reference closed-loop dynamics. By substituting equation (32) in the dynamics of the observation error, i.e., $\dot{e} = k_L(\dot{e}_t - \dot{e}_{t_f})$, one obtains:

$$\dot{e} = -k_L e - k_L K_0 \Lambda_K (\Delta \alpha_1 \omega + \Delta \alpha_2 \tau_b + \Delta \sigma + \Delta \alpha_3 f(\omega)). \quad (33)$$

With respect to (25), the only difference is the term $K_0 A_0 e$ that is missing from (33). Note that the negative sign in front of the mismatch term in (33) is due to the convention used in defining e_t but the contradiction is resolved thanks to the negative sign in the adaptation laws (26)-(29). Therefore, the two solutions would match if the observer gain were selected as $L = -k_L I_3$ in (25) and the term $-\frac{K_0 A_0}{k_L} e$ were included in the definition of e_{t_f} (32). It is worth remarking that for a sufficiently large gain k_L , which is expected when seeking high performance, the two approaches yield the same observation error dynamics.

\mathcal{L}_1 augmentation design of attitude control

In this section a predictor-based \mathcal{L}_1 adaptive control design is presented for comparison purposes. Consider again equation (9) and add and subtract the nominal part of the system:

$$\begin{aligned} \dot{\omega} &= K_0 \Lambda_K ((A_0 + A_\delta) \omega + \tau_c + \sigma) + (H_0 + H_\delta) f(\omega) \\ &\quad \pm K_0 (A_0 \omega + \tau_b) \\ &= \underbrace{K_0 (A_0 \omega + \tau_b)}_{\text{Nominal part}} + K_0 (\alpha_1 \omega + \alpha_2 \tau_b + \Lambda_K \tau_a + \sigma + \alpha_3 f(\omega)) \end{aligned} \quad (34)$$

where

$$\alpha_1 := (\Lambda_K - I_3) A_0 + \Lambda_K A_\delta \quad (35)$$

$$\alpha_2 := \Lambda_K - I_3 \quad (36)$$

$$\alpha_3 := K_0^{-1} (H_0 + H_\delta) \quad (37)$$

$$\sigma := \Lambda_K \sigma. \quad (38)$$

Further, we can make use of the fact that the actuator can be modeled as an uncertain input gain, and thus rewrite the previous equation as

$$\dot{\omega} = K_0 (A_0 \omega + \tau_b) + K_0 (\alpha_1 \omega + \alpha_2 \tau_b + \lambda u_a(t) + \sigma + \alpha_3 f(\omega)), \quad (39)$$

where λ is a parameter used in \mathcal{L}_1 adaptive control to model the uncertain input gain¹⁹. Notice that Λ_K is included in λ .

Design of the filter $C(s)$

We know^{17,19} that we can design the filter $C(s)$ so that the reference system is stabilized. In our case the reference system is given by

$$\begin{aligned} \dot{\omega} &= K_0 (A_0 \omega + \tau_b) + K_0 (\alpha_1 \omega + \alpha_2 \tau_b + \lambda u_a \\ &\quad + \sigma + \alpha_3 f(\omega)) \\ u_a &:= -\frac{1}{\lambda} C(s) (\alpha_1 \omega + \alpha_2 \tau_b + \sigma + \alpha_3 f(\omega)) \end{aligned} \quad (40)$$

and $C(s)$ needs to be a proper stable filter with DC-gain $C(0) = 1$. Further, the reference system should be stable for all the possible unknown dynamics of the actuator. Let F_Δ denote the set of possible dynamics of the actuator, with $G(s) \in F_\Delta$, then $C(s)$ has the following structure:

$$C(s) := \frac{kF(s)D(s)}{1 + kF(s)D(s)} \quad (41)$$

with $F(s) \in F_\Delta$, $k > 0$ user chosen and $D(s)$ selected as

$$D(s) := \frac{1}{s} \quad (42)$$

to satisfy the assumption of DC-gain $C(0) = 1$. The actuator was modelled according to equation (11), whilst the nominal control is given by the output of a PID controller $R_{\text{PID}}(s)$

$$\tau_b := G(s) R_{\text{PID}}(s) (r - \omega), \quad (43)$$

with r being the reference signal. Let then

$$R(s) = G(s) R_{\text{PID}}(s), \quad (44)$$

and

$$\begin{aligned} H(s) &:= (sI - K_0 A_0 + K_0 R(s))^{-1} K_0, \\ M(s) &:= 1 - C(s) \end{aligned} \quad (45)$$

from which it follows that

$$\begin{aligned} \dot{\omega} &= H(s) R(s) r(s) \\ &\quad + H(s) M(s) (\alpha_1 \omega + \alpha_2 R(s) (r - \omega) \\ &\quad + \tilde{\sigma} + \alpha_3 f(\omega)). \end{aligned} \quad (46)$$

Next, define

$$\begin{aligned} G_1(s) &:= H(s) R(s) + H(s) M(s) R(s) \alpha_2, \\ G_2(s) &:= H(s) M(s) R(s) \end{aligned} \quad (47)$$

and $G_3(s) := H(s) M(s)$. If the filter gain k in (41) is selected such that $G_d(s) := (I_3 + G_2(s) \alpha_2 - G_3(s) \alpha_1)^{-1}$ is a stable transfer function for all possible values of α_1, α_2 , then the reference system is stable. It can be shown¹⁷ that a sufficient condition for stability is the \mathcal{L}_1 norm of $G_d(s)$ be finite. Hence, an upper bound on the value of k can be found by checking up to which value $\|G_d(s)\|_{\mathcal{L}_1} < \infty$.

Predictor model and control law

Based on the expression of the plant model given in equation (39) the predictor model

$$\begin{aligned} \dot{\hat{\omega}} &= K_0(A_0\hat{\omega} + \tau_b) \\ &+ K_0(\hat{\alpha}_1\omega + \hat{\alpha}_2\tau_b + \hat{\lambda}u_a(t) + \hat{\sigma} + \hat{\alpha}_3f(\omega)) \quad (48) \\ &+ Le \end{aligned}$$

is used, where $\hat{\alpha}_1, \hat{\alpha}_2, \hat{\lambda}, \hat{\sigma}, \hat{\alpha}_3$ are the estimates of $\alpha_1, \alpha_2, \lambda, \sigma, \alpha_3$.

Further, let again L be a Hurwitz matrix, added to choose the convergence rate of the error dynamics, where the error is defined as $e := \hat{\omega} - \omega$, then, based on that, the error dynamics is modeled by

$$\begin{aligned} \dot{e} &= (K_0A_0 + L)e \\ &+ K_0(\Delta\alpha_1\omega + \Delta\alpha_2g_b) \quad (49) \\ &+ \Delta\lambda u_a(t) + \Delta\sigma + \Delta\alpha_3f(\omega). \end{aligned}$$

Finally, the adaptive control law is defined as

$$\begin{aligned} u_a(s) &:= -kD(s)\eta(s), \quad (50) \\ \eta(s) &:= \hat{\alpha}_1\omega + \hat{\alpha}_2g_b + \hat{\lambda}u_a + \hat{\sigma} + \hat{\alpha}_3f(\omega), \end{aligned}$$

where k and $D(s)$ are chosen as discussed in the previous subsection.

Adaptive laws

Based on the error equation (49), the adaptive laws

$$\dot{\hat{\alpha}}_1 := \text{Proj}(\hat{\alpha}_1, -\Gamma_1\omega e^T PB) \quad (51)$$

$$\dot{\hat{\alpha}}_2 := \text{Proj}(\hat{\alpha}_2, -\Gamma_2\tau_b e^T PB) \quad (52)$$

$$\dot{\hat{\alpha}}_3 := \text{Proj}(\hat{\alpha}_3, -\Gamma_3f(\omega)e^T PB) \quad (53)$$

$$\dot{\hat{\lambda}} := \text{Proj}(\hat{\lambda}, -\Gamma_4u_a e^T PB) \quad (54)$$

$$\dot{\hat{\sigma}} := \text{Proj}(\hat{\sigma}, -\Gamma_5e^T PB), \quad (55)$$

are used. The initial condition of the uncertain parameter associated with λ , which is the equivalent gain of the propellers dynamics, is $\hat{\lambda}(0) = I_3$. The other initial conditions are the same used for the MRAC scheme.

Quadrotor and baseline controller

The considered quadrotor, depicted in Figure 1, is a lightweight custom model with a distance of 160mm between opposite rotor axes and an overall take-off weight of about 230g. The relevant parameters are reported in Table 1. The flight control unit is a Pixfalcon board, an open autopilot shield suitable for remotely controlled vehicles such as multirotors and fixed wing aircraft. It is equipped with a 3 axes accelerometer, a 3 axes gyroscope, a magnetometer and a pressure sensor. The firmware running on the Pixfalcon board is the open-source software PX4 Pro Autopilot. The firmware features attitude and position controllers and estimators, and has been customized to allow replacing the baseline attitude controller with a user-defined controller.

The baseline controller implemented in the PX4 firmware has a cascade architecture as shown in Figure 2; for each



Figure 1. Quadrotor used for the tests.

Variables	Value
Frame Config.	X
Propellers	Gemfan Bullnose 3055 3 blade
Arm length b	80 mm
Take-off weight m	230 g
Motors	QAV1306-3100kV brushless
ESC	ZTW Spider series 18A
Battery	Turnigy nano-tech 950mAh LIPO

Table 1. Main quadrotor parameters.

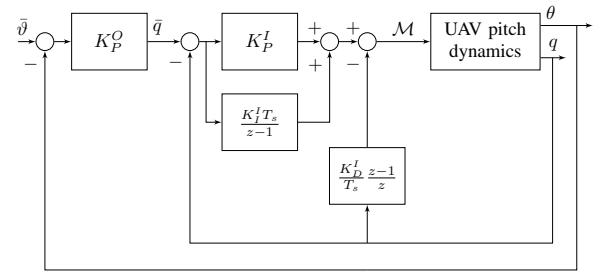


Figure 2. Baseline attitude controller block diagram (pitch axis).

axis, a PID inner loop tracks the desired angular rate, which is fed by a proportional outer loop on the attitude angle. The superscript I indicates the inner loop gains, while the superscript O is for the outer loop gains. The baseline controller gains have been tuned to achieve satisfactory performance in terms of response to pilot commands, and are reported in Table 2 for the three axes.

Table 2. Baseline controller gains.

Axis	K_P^O	K_I^I	K_D^I	K_P^O
Roll	0.1	0.21	0.003	13
Pitch	0.14	0.21	0.003	13
Yaw	0.06	0.05	0.001	4

Experimental results

Both the observer-based MRAC and \mathcal{L}_1 adaptive control laws were experimentally tested in flight. The cascade PID controller architecture described in the previous section was used as a baseline to show performance improvement of

the two adaptive laws in terms of capability of rejecting disturbances.

The adaptive control laws were implemented and validated on all the three axes of roll, pitch and yaw; though, only results related to the pitch axis will be presented, due to space limitations. Bounds on the adaptation coefficients are shown in Table 3; they are the same for both the MRAC and \mathcal{L}_1 adaptive laws (except for the bound on λ which is only applicable to \mathcal{L}_1). Similarly, gains on the adaptation coefficients are reported in Table 4; it can be noticed that, where applicable, the gains of the \mathcal{L}_1 law are larger than the MRAC ones: this is made possible by the presence of the filter in (50). As for the observer gain, a value of $L = 150I_3$ was chosen for the MRAC law while a higher value of $L = 300I_3$ was selected for the \mathcal{L}_1 law. As for the \mathcal{L}_1 filter constant, $k = 25$ has been chosen. Both the bounds and the gains values were tuned by trial and error. Note that for rotations occurring about one principal axis the $f(\omega)$ term is negligible, therefore the contribution of α_3 has not been included in (19) and (50).

Table 3. Bounds on the adaptation laws coefficients.

Coefficient	Value
α_1	10^{-2}
α_2	10^{-1}
λ	0.3
σ	0.2

Table 4. Gains on the adaptation laws coefficients.

Coefficient	Gain (MRAC)	Gain (\mathcal{L}_1)
α_1	10^{-3}	1
α_2	10^{-1}	10
λ	-	10
σ	2×10^{-2}	10^{-1}

An experiment was designed to verify the ability of the adaptive control laws to quickly recover level attitude in the case a disturbance occurs on the actuators. The experiment consists in taking the quadrotor to hovering; then, an artificial disturbance on the actuators is injected, *i.e.*, a step disturbance with an amplitude of half the maximum available control moment (in this case, the maximum pitch moment \bar{m}) is summed to the control moment u , downstream the controller:

$$u_{cmd} = u + \Delta u \quad (56)$$

$$\Delta u := \begin{bmatrix} 0 & 0.5\bar{m} & 0 \end{bmatrix}^T \quad (57)$$

so that the actual commanded actuator control action is u_{cmd} .

This experiment is representative of the effect of a (partial or total) loss of throttle on one or more motors, as this would produce a loss of thrust, which in turns produces a disturbance moment about the body axes of the quadrotor.

Figure 3 shows the pitch angle and pitch angular rate responses to the injected disturbance on the pitch axis. The disturbance occurs at time instant $t = 0$. It can be noticed that

the two adaptive control laws outperform the baseline law in terms of attitude angle disturbance reaction time t_R , which is defined as the time needed to recover the initial attitude angle θ_0 within a range of $\pm 1.5\text{deg}$. The disturbance reaction times for the three control laws are reported in Table 5, along with the peak e_{PK} and the RMS e_{RMS} of the error e_θ , where e_θ is defined as the difference between the pitch angle θ and its value θ_0 before the disturbance injection, namely:

$$e_\theta := \theta - \theta_0. \quad (58)$$

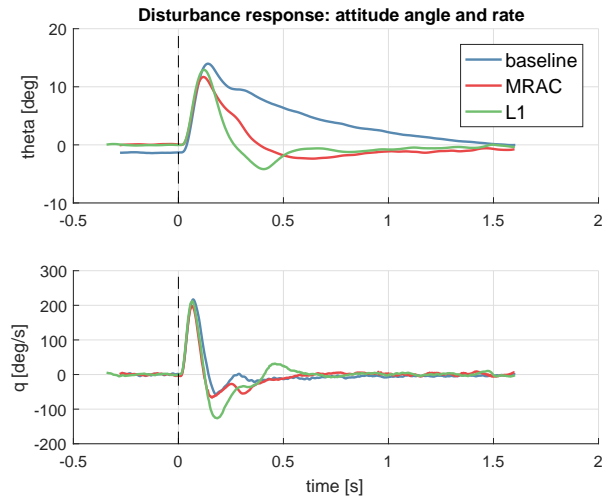


Figure 3. Pitch angle and angular rate: response to input disturbance (comparison between baseline, MRAC and \mathcal{L}_1).

Table 5. Performance metrics: pitch response to input disturbance (in brackets the relative reduction with respect to baseline).

Control law	t_R [s]	e_{PK} [deg]	e_{RMS} [deg]
baseline	1.496	15.3	6.19
MRAC	0.340 (-77.3%)	11.6 (-24.1%)	3.21 (-48.2%)
\mathcal{L}_1	0.242 (-83.8%)	12.9 (-15.6%)	3.11 (-49.7%)

It can be noticed that, in all the cases, the pitch angle undergoes an initial sudden variation; then, control comes into play and the pitch angle returns to the initial value. In the baseline case, the angle slowly returns to zero attitude always remaining positive, while in the case of the two adaptive laws the attitude angle quickly returns to zero and during the transient also reaches negative values; this turns into an interesting “braking” effect of the quadrotor, and results in a small displacement from its initial position. The \mathcal{L}_1 adaptive law achieves a better disturbance reaction time with respect to MRAC.

As for the peak angle, the two adaptive laws achieve a smaller peak with respect to the baseline, with MRAC performing better than \mathcal{L}_1 . The RMS of the error is also reduced with respect to the baseline, in the case of the two adaptive laws.

Figure 4 shows the respective control actions for the three control laws; the control action is dimensionless, *i.e.*, a value

of $m = 1$ indicates the maximum control moment which can be produced about the pitch axis. The effect of adding the step disturbance downstream the controller can be noticed in that the steady-state value of the control action response counterbalances the disturbance (with equal magnitude and opposite value). Despite looking very similar, the three control actions actually produce very different results in term of pitch angle response; one difference between the baseline and the adaptive laws can be seen in the steady-state behaviour of the control action response, which has a slightly larger value in the case of the baseline law, resulting in the slow decrease of the attitude angle depicted in Figure 3. The RMS of the control action u_{RMS} for the three control laws is reported in Table 6. The RMS is similar in all the cases, showing that the control energy employed is comparable; the RMS in the adaptive laws is slightly larger than the baseline case.

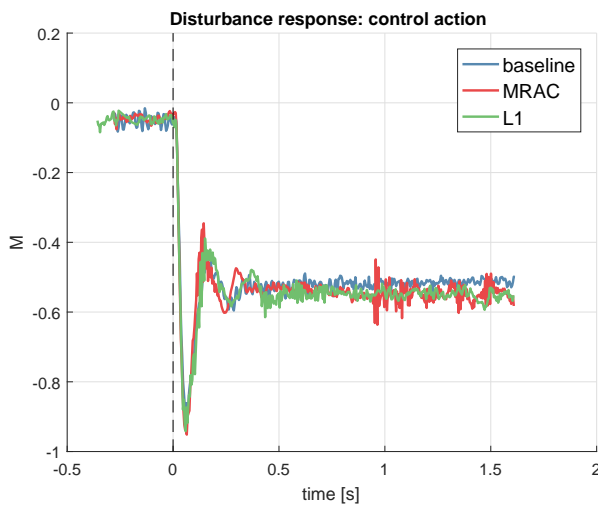


Figure 4. Pitch control action: response to input disturbance (comparison between baseline, MRAC and \mathcal{L}_1).

Table 6. Performance metrics: control action response to input disturbance.

Control law	u_{RMS}
baseline	0.491
MRAC	0.509
\mathcal{L}_1	0.518

The contribution of the adaptation law to the control action is shown in Figures 5 and 6 respectively, for the MRAC and \mathcal{L}_1 adaptive laws, where the control action has been split into its components u_a and u_b (see equation (12)).

The adaptive contributions (namely, u_a) from MRAC and \mathcal{L}_1 have been compared and shown in Figure 7; it can be noticed that \mathcal{L}_1 presents a more prompt response of the adaptive contribution as the disturbance shows up.

Finally, the response of the adaptive coefficients is shown in Figures 8 and 9 respectively for the MRAC and \mathcal{L}_1 control laws; the coefficients (solid lines) are shown along with their saturation bounds (dashed lines). Notice that these plots consider a wider time horizon than the previous plots. In these experimental runs, the disturbance is injected and removed several times. The presence of the disturbance is

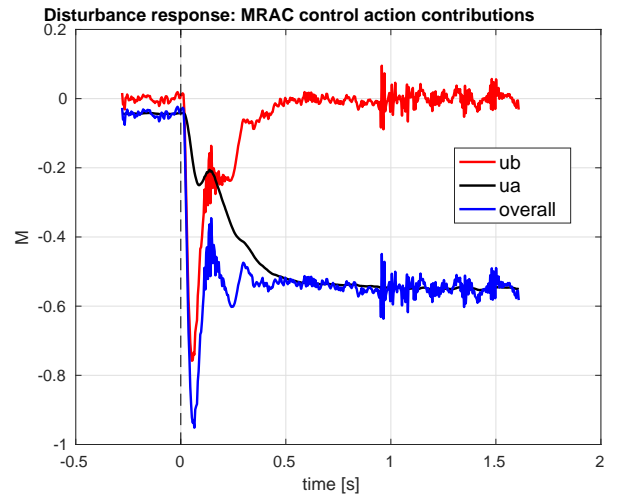


Figure 5. Contributions of MRAC adaptive law: response to input disturbance.

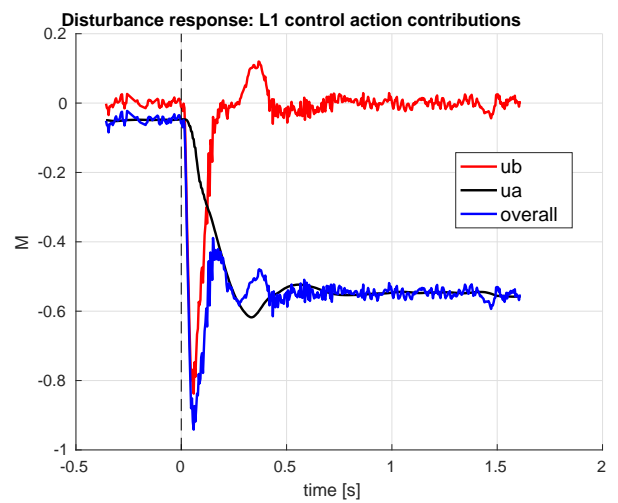


Figure 6. Contributions of \mathcal{L}_1 adaptive law: response to input disturbance.

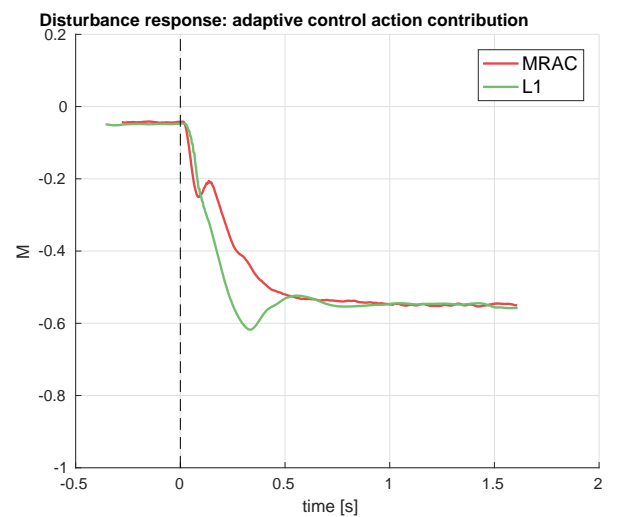


Figure 7. Adaptive contributions of MRAC and \mathcal{L}_1 : response to input disturbance.

well represented by the plot of σ , which can be interpreted as an estimate of the external disturbance as it varies with time.

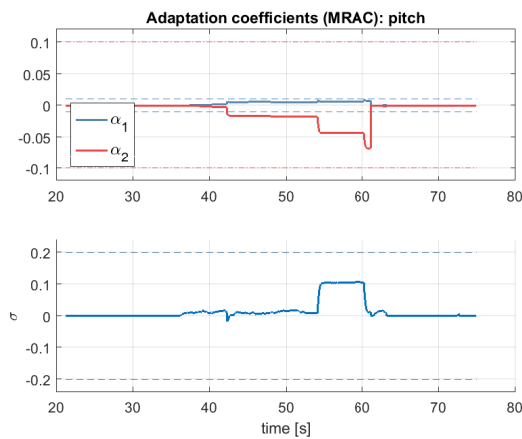


Figure 8. Adaptation coefficients: MRAC.

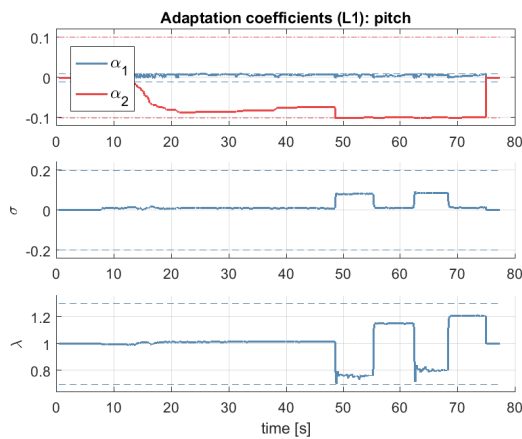


Figure 9. Adaptation coefficients: \mathcal{L}_1 .

Conclusions

In this paper we proposed an adaptive augmentation scheme that can be implemented on top of an existing controller and that has shown improvements in terms of disturbance rejection performance, with only a small increase of the required control power. A novel MRAC scheme, that includes an observer to estimate the uncertainties, has been presented and compared to similar approaches. The proposed design showed superior performance with respect to the nominal controller when operated in the presence of significant disturbances. We tested the observer-based MRAC controller on a quadrotor UAV and the experimental results confirmed the overall performance improvement with respect to the baseline controller. Furthermore, similar performance were obtained with respect to a predictor-based \mathcal{L}_1 controller. In conclusion, the adaptive laws developed in this work offers an increased robustness to parametric uncertainties and they are effective in mitigating a loss-of-thrust like anomaly compared to the nominal controller alone.

References

- Invernizzi D, Lovera M and Zaccarian L. Geometric trajectory tracking with attitude planner for vectored-thrust VTOL UAVs. In *2018 Annual American Control Conference (ACC)*. pp. 3609–3614.
- Ghaffar AA and Richardson T. Model reference adaptive control and LQR control for quadrotor with parametric uncertainties. *Int Journal of Mechanical, Aerospace, Industrial, Mechatronic and Manufacturing Eng* 2015; 9(2): 244–250.
- Dydek ZT, Annaswamy AM and Lavretsky E. Adaptive control of quadrotor UAVs in the presence of actuator uncertainties. *AIAA Infotech Aerospace* 2010; : 20–22.
- Lavretsky E and Wise K. *Robust and Adaptive Control With Aerospace Applications*. Springer London, 2013.
- Lavretsky E et al. Combined/composite model reference adaptive control. *IEEE Transactions on Automatic Control* 2009; 54(11): 2692.
- Dydek ZT, Annaswamy AM and Lavretsky E. Adaptive control of quadrotor UAVs: A design trade study with flight evaluations. *IEEE Transactions on Control Systems Technology* 2013; 21(4): 1400–1406.
- Gibson TE, Annaswamy AM and Lavretsky E. On adaptive control with closed-loop reference models: transients, oscillations, and peaking. *IEEE Access* 2013; 1: 703–717.
- Beard RW, Knoebel NB, Cao C et al. An l_1 adaptive pitch controller for miniature air vehicles. In *AIAA Guidance, Navigation, and Control Conference, Keystone, CO*.
- Wang J, Patel V, Woolsey CA et al. L_1 adaptive control of a UAV for aerobiological sampling. In *2007 American Control Conference*. IEEE, pp. 4660–4665.
- Michini B and How J. L_1 adaptive control for indoor autonomous vehicles: design process and flight testing. In *Proceeding of AIAA Guidance, Navigation, and Control Conference*. pp. 5754–5768.
- Mallikarjunan S, Nesbitt B, Kharisov E et al. L_1 adaptive controller for attitude control of multirotors. In *AIAA Guidance, Navigation and Control Conference, Minneapolis, AIAA-2012-48312012*.
- Chowdhary G, Wu T, Cutler M et al. Experimental results of concurrent learning adaptive controllers. In *AIAA Guidance, Navigation, and Control Conference (GNC), (Minneapolis, MN), AIAA*.
- Chowdhary GV and Johnson EN. Theory and flight-test validation of a concurrent-learning adaptive controller. *Journal of Guidance, Control, and Dynamics* 2011; 34(2): 592–607.
- Madani T and Benallegue A. Adaptive control via backstepping technique and neural networks of a quadrotor helicopter. In *17th IFAC World Congress, Seoul, South Korea*.
- Johnson EN and Kannan SK. Adaptive trajectory control for autonomous helicopters. *Journal of Guidance, Control, and Dynamics* 2005; 28(3): 524–538.
- Russo A, Invernizzi D, Giurato M et al. Adaptive augmentation of the attitude control system for a multirotor UAV. In *7th European Conference for Aeronautics and Space Sciences, 2017*.
- Russo A. *Adaptive control of multirotor UAVs*. Master's Thesis, Politecnico di Milano, Italy, 2017.
- Kim S and Kim Y. Mismatch-observer based model reference adaptive control for transient performance improvement of aircraft. In *AIAA Guidance, Navigation, and Control Conference*. p. 1504.
- Hovakimyan N and Cao C. *L_1 adaptive control theory: guaranteed robustness with fast adaptation*, volume 21. Siam, 2010.